A novel smart rad-hard fast detection system for Radioactive Ion Beam Tagging and Diagnostics

Luis Acosta[1], Carmen Altana[2], Giuseppe Cardella[3], Andrea Castoldi[4,5], Michele Costa[2], Enrico De Filippo[3], Elena Geraci[6,3], Brunilde Gnoffo[3], Chiara Guazzoni[4,5,*], Cettina Maiolino[2], Nunzia Simona Martorana[3], Andrea Naggi[4,5], Angelo Pagano[3], Emanuele Vincenzo Pagano[2], Sara Pirrone[3], Giuseppe Politi[6,3], Fabio Risitano[7,3], Francesca Rizzo[6,3], Antonio Domenico Russo[2], Paolo Russotto[2], Marina Trimarchi[7,3], Salvo Tudisco[2]

[1]Instituto de Física, Universidad Nacional Autónoma de México, Mexico
[2]LNS-INFN, Italy
[3]INFN, Sezione di Catania, Italy
[4]Politecnico di Milano, Dip. Elettronica, Informazione e Bioingegneria, Italy
[5]INFN, Sezione di Milano, Italy
[6] Dipartimento di Fisica e Astronomia, Universita' degli Studi di Catania, Italy
[7]Dip. di Scienze MIFT Universita' di Messina, Italy

(*) chiara.guazzoni@mi.infn.it

***Abstract*— Radioactive Ion Beams (RIBs) of large intensity (10^6 pps or higher) are at the frontier in nuclear physics. We designed a novel detection system for RIBs diagnostics and tagging based on Silicon Carbide detectors and on custom frontend electronics ready to be coupled with a Real Data Management Unit. The full detection system is designed to measure the spatial distribution of the beam intensity and trajectory with sufficient spatial resolution (of the order of 1-2 mm). In addition, the detection system has to determine the RIB composition that can be obtained from the joint measurement of the energy loss (ΔE) of the ions passing through the sensors and the time of flight between two sensors or with respect to a given reference signal as the Radio-Frequency signal of a Cyclotron. In this paper we present the full design of the proposed system together with the results of the first experimental qualification of the first mini-prototype. The paper also shows the steps towards the final detection system, housed in a DN160 spherical cross and able to cover an active area of 30 mm × 60 mm.**

***Keywords*— Radioactive Ion Beams, Particle Tagging, Beam Monitor, Fast Electronics**

I. Introduction

RADIOACTIVE Ion Beams (RIBs) [1], [2], [3] of large intensity (10^6 pps or higher) are at the frontier in nuclear physics and are available since one decade in different facilities [4], [5], [6] and new ones are presently under construction [7] to deliver intense RIBs to the nuclear physics community and to produce radiopharmaceuticals.

The exotic nuclei (short-lived nuclear species) are a unique tool to investigate properties of nuclei and nuclear matter under extreme conditions and have proven to be very effective in unveiling the fundamental properties of the still not well-known nuclear force. RIBs allow the study of reactions of fundamental importance for the nucleosynthesis of elements in the universe.

Radioactive isotopes produced in RIBs facilities find a relevant application in the medical field as radiopharmaceutical and innovative techniques foresee the use of radioactive isotopes, such as ^{11}C, in hadron therapy [8].

The tuning and transport of the radioactive beam are of critical importance to deliver high-quality beams, but they represent a time-consuming process and require dedicated diagnostics and tagging devices measuring different RIBs features in combination with skilled personnel. The same devices should be capable of operation in radioactively activated environments because of the expected high direct and background irradiation and to sustain several experiments per year.

To this aim, we are developing a dedicated instrument [10] for the diagnostics and the tagging of RIBs along the transport line based on an array of Silicon Carbide (SiC) diodes [11], readout by an optimized fast frontend electronics and ready to be coupled with a smart DAQ with Data Real-Time Management capabilities and a dedicated software layer implementing Artificial Intelligence and machine learning techniques.

The system is originally designed to cope with the characteristics of a new fragment separator, FRAgment In-fligth SEparator (FraISe) [7], [12], [13], [14], being built at Laboratori Nazionali del Sud of INFN in Catania (Italy), as part of the upgrade of the facility [15] to push the rate of production of high luminosity stable and radioactive beams.

The facility will produce RIBs exploiting the in-flight technique based on the fragmentation of the primary beam that

impinges on light Be or C targets. FraISe makes use of light and medium mass primary beams, having power limited to ≈ 2–3 kW for radioprotection issues, leading to RIBs, whose intensities vary in the range of ≈ 10^3–10^7 pps [14], for nuclei far from and close to the stability valley, respectively. FraISe aims at providing high-intensity and high-quality RIBs for nuclear physics experiments, also serving to interdisciplinary research areas, such as medical physics. The improvement in beam intensity opens the way to more precise studies on nuclei close to stability and allows the extension of the investigations also to nuclei far from stability.

Several beam diagnostic/tagging devices are needed within FraISe: i) and ii) within the fragment separator in two points (degrader & exit slits), where there is the need during beam optimization of a point-to-point measurement of the cocktail intensity, of its relative composition, of the energy distribution, of the 2D profile, and of the angular distribution; and during data taking of monitoring the beam properties, of measuring the start time for the event-by-event ToF/energy measurement for particle identification; iii) in the final set-up point (measurement chamber), where there is the need of event-by-event tagging of the cocktail beam and of trajectory measurements.

We chose a one device-fits-all approach. The modularity and the flexibility of the system make it suitable both for beam diagnostics and for particle tagging not only for the aforementioned needs in FraISe but also in different fragment separators and facilities.

In this paper we present the full design conception of the proposed system together with the results of the first experimental qualification of the first mini-prototype. The paper is organized as follows. Section II illustrates the architecture of the full tagging system. Section III describes the first developed workhorse, called mini-prototype and section IV is devoted to the first experimental qualification of the first mini-prototype. Section V ends with conclusions and gives an .

II. Architecture of the Full Tagging System

The full detection system [9], [10] is designed to be housed in a DN160 spherical cross to be inserted along the beam path. Eight monolithic detector tiles of 1.5 cm × 1.5 cm 4H-SiC diodes will be placed side-by -side to cover the detection active area of about 30 mm × 60 mm as required to reconstruct typical RIBs profiles in the high dispersion point of the fragment separator. SiC has been chosen due to its superior properties with respect to Si [16]. The detector thickness is about 100 µm, as a compromise among mechanical strength, epitaxial layer growable thickness and readout node capacitance. SiC detectors are segmented in square pads of 5 mm side as a tradeoff between particle rate, power budget and required resolution, resulting in 72 readouts elements. Fig. 1a shows a simplified CAD view of the final tagging system housed in its spherical DN160 cross to be located along the beam path. The beam is coming orthogonal to the figure. Fig. 1b shows a closer view of the detection area. Wire bondings connect each individual pad to the corresponding readout channel. Less than 11mm difference in the bonding wires length cause a negligible dispersion of the parasitic capacitance do not cause a relevant dispersion in the output node capacitance.

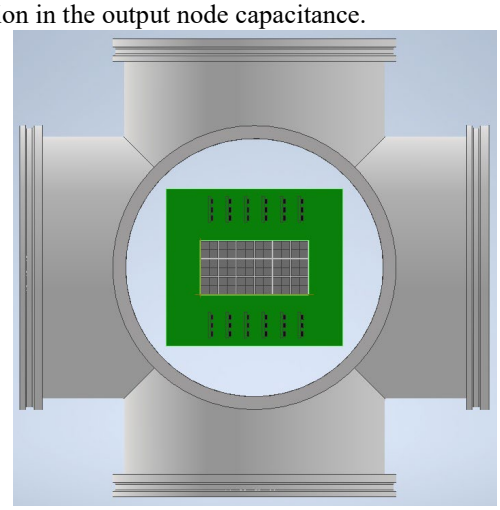

(a)

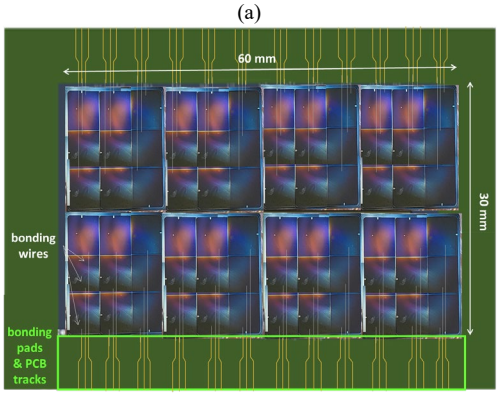

(b)

Fig. 1. a) CAD view of the final tagging system housed in its spherical DN160 cross to be located along the beam path. b) closer view of the detector active area, where 8 monolithic detector tiles are placed side-by-side to cover the 30 mm × 60 mm detection area.

Each detection unit is readout by a dedicated frontend in charge preamplifier configuration with fast decay to cope with the foreseen particle flux up to 10^7 pps on the full detection area. A selected, high-performance operational amplifier plays the role of forward gain stage. A fully differential amplifier is responsible of line driving and additional filtering if needed. Ref. [17] contains a detailed description of the frontend electronics architecture.

III. The First Mini-Prototype Structure

In order to experimentally qualify the system performance, we assembled a mini-prototype of the final tagging system, featuring 1 cm^2 active area. The detector carrier is able to house a 1 cm^2 single die segmented in 4 detection units or up to 4 dies, with an active area of 25 mm^2 per single unit. Fig.2a and Fig.2b show the photo of two of the different detector prototypes available, a 25 mm^2 detection unit and a monolithic 1 cm^2 active area detector segmented in four individual detection units.

We designed two different substrates to be used as detector carriers (motherboards) and to house the frontend electronics. Fig.2c and Fig.2d shows the two different motherboards. The

first developed carrier is the safest one and allows to easily glue and bond even non-monolithic arrays. It is designed with a dedicated stack-up to reduce the thickness in the detector area to the minimum (300 µm) so as to minimize the material budget along the beam path. The second one is closer to the final design as it has a milled area in correspondence of the detector active area to remove all the material budget and work in full transmission mode. The gluing bridge in the center of the transmission window features the minimum width for the technology that is 600 µm and will be used also to probe its impact on the quality of the identification matrices as it is unavoidable also in the final system to mount the individual dies.

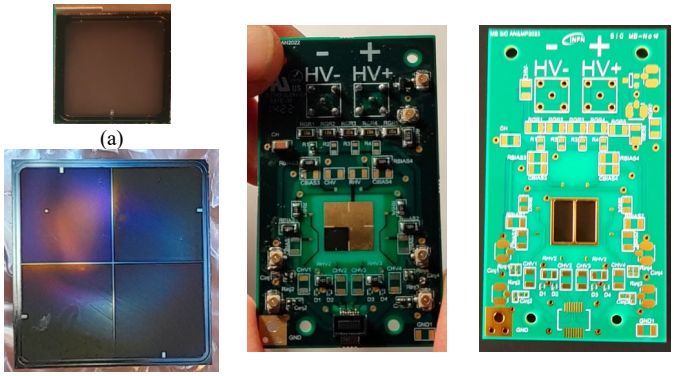

Fig. 2. a) Photo of one 5 mm × 5 mm active area detector prototype. b) Photo of one monolithic detector prototype 1cm^2 active area, segmented in 4 independent detection units. c) Photo of one detector prototype 5 mm × 5 mm active area mounted on the motherboard with minimized material budget along the beam path. d) Photo of the motherboard designed to allow the mounting of different detectors prototypes (up to 1 cm^2 die size) in transmission mode.

A 4-channel custom frontend board with the same configuration of the final system is directly coupled with the detector motherboard by means of the 0.50mm Pitch SlimStack Plug visible at the lowest side of the motherboard in the middle of the two fixing holes. The signal coming from the frontend electronics in charge preamplifier configuration is driven to the outer world by means of a fully-differential line driver through a dedicated high-integrity Samtec HSEC8-113-01-S-DV-A-K connector. Fig. 3 shows the photo of the 4-channel frontend board. Individual U.FL-R-SMT-1(10) coaxial connectors allow probing also the single-ended output of the charge preamplifier.

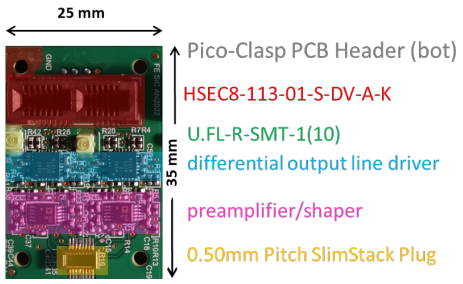

Fig. 3. Photo of the custom 4-channels frontend board with the main components highlighted.

IV. Experimental Qualification of the First Mini-Prototypes

We performed a detailed qualification of the individual system components prior to assembling the first mini-prototypes. Ref. [10] and [17] present and discuss the results of this qualification. We report here the results of the first qualification of one mini-prototype.

In order to qualify the system response, we probed the output waveform as a function of the applied reverse bias upon electrical injection exploiting a dedicated injection line through a 1 pF injection capacitance connected to the charge preamplifier virtual ground. Fig. 4a shows the corresponding output waveforms. Fig. 4b shows the maximum value, minimum value and amplitude of the output waveform as a function of the applied reverse bias voltage. The vertical line indicates the full depletion voltage as resulting for the considered prototype from independent CV measurements [10]. As it can be noticed above 200 V reverse bias, when the detector capacitance drops well below 50 pF [10], 6the output response follows the expected behavior with no overshoot, however the output waveform maximum, minimum and amplitude saturate to the target value (indicated by the corresponding horizontal line), only above depletion.

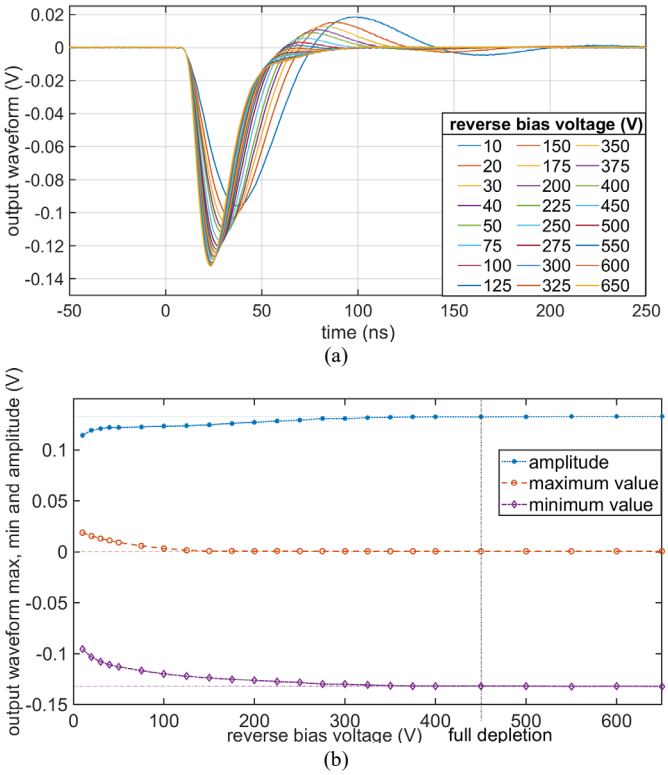

Fig. 4. a) Output waveforms upon electrical injection as a function of the applied reverse bias voltage in the case of the setup with minimized material budget. b) Maximum value, minimum value and amplitude of the output waveform as a function of the applied reverse bias voltage. The vertical line indicates the full depletion voltage as resulting for the considered prototype from independent CV measurements [10].

We illuminated the detector with a 3kBq mixed-nuclei α source (^{239}Pu, ^{241}Am, ^{244}Cm). Also in this case we acquired the output waveforms as a function of the applied reverse bias in order to better investigate the system performance, including also the charge collection process. Fig. 5 shows the corresponding output waveforms. Output waveforms as a function of the applied reverse bias in the case of the setup with minimized material budget in the case of alpha particle

detection from the mixed nuclei source. We chose always the same alpha energy, corresponding to the ^{244}Cm alpha energy (5806 keV).

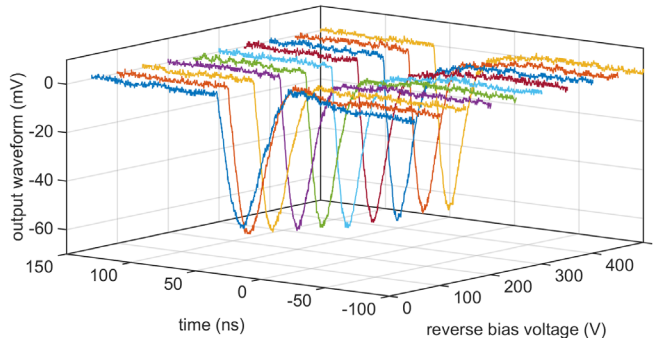

Fig. 5. Output waveforms as a function of the applied reverse bias in the case of the setup with minimized material budget in the case of alpha particle detection from the mixed nuclei source. We chose always the same alpha energy, corresponding to the 244Cm alpha energy (5806 keV).

We directly digitized the output waveforms with a High Resolution Oscilloscope from Teledyne LeCroy (12 bits vertical resolution). From the acquired waveforms we performed a preliminary qualification of the spectroscopic performance of the system, limited by operation in air. Fig.6 shows the measured spectrum in air when the waveforms are filtered with an 11 taps digital filter. The quality of the spectrum is affected by operation in air, however the measured resolution at the pulser line (not spoiled by operation in air) is 60 keV FWHM well within required specifications.

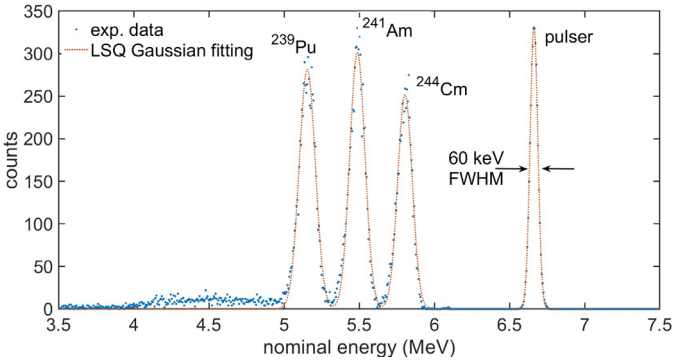

Fig. 6. Measured spectrum in air when the detector is illuminated by a mixed-nuclei α source. The measured resolution at the pulser line is 60 keV FWHM. The quality of the spectrum is degraded by operation in air.

V. Conclusions

This paper presented the results of the first experimental qualification of the first mini-prototype of the designed tagging system for the new FraISe facility now in its final phase of construction. The mini-prototype features a 1 cm^2 active area and allows probing all the feature of the final system. The opamp based fast frontend is fully developed and qualified. The system performance was experimentally assessed in the lab with electrical injection and with a mixed nuclei alpha radioactive source. The measured pulse rise time is sufficiently faster, below 10 ns for the 10%-90% rise time and subject to further improvement. The measured INL is below 0.2% up to 50 MeV input signal and we measured an energy resolution of 60 keV FWHM in air with the fast electronics,

Given the positive and promising results of the qualification in the lab the mini-prototype will be qualified with stable beams in the next months, pending the availability of the first radioactive beams of FraISe. This test will give precious results for the design and assembly of the final system. The mini-prototype will be populated also with the monolithic array of 2 × 2 SiC diodes in order to investigate charge sharing and cross-talk.

Acknowledgment

This work was supported by INFN, Istituto Nazionale di Fisica Nucleare in the framework of the CHIRONE experiment and by Politecnico di Milano, with the visiting scientists initiative.

The authors gratefully acknowledge the precious contribution of Mattia Pozzi (Politecnico di Milano) in the PCB design and the valuable qualified professionalism of Sergio Masci in the detector gluing and bonding.

References

[1] K. Hagino, I. Tanihata and H. Sagawa, Exotic Nuclei Far from the Stability Line, In: Henley, E.M., Ellis, S. D. (ed.) 100 Years of Subatomic Physics. World Scientific, Singapore, vol. 231, 2013.
[2] I. Tanihata, “Nuclear structure studies from reaction induced by radioactive nuclear beams”, Prog. Part. Nucl. Phys., vol. 33, pp. 505-573, 1995.
[3] EPJA Focus Point on Rewriting Nuclear Physics textbooks: 30 years with radioactive ion beam physics, Eur. Phys. J. Plus 131, 2016.
[4] Y. Blumenfeld, T. Nilsson, P. van Duppen. “Facilities and methods for radioactive ion beam production”, Physica Scripta, pp.14023, 2013.
[5] K.-H. Schmidt, E. Hanelt, H. Geissel, G. Münzenberg, J.P. Dufour, “The momentum-loss achromat — A new method for the isotopical separation of relativistic heavy ions”, Nucl. Instrum. Meth. A, vol. 260, pp. 287-303, 1987.
[6] R. Anne and A.C. Mueller, “LISE 3: a magnetic spectrometer—Wien filter combination for secondary radioactive beam production”, Nucl. Instrum. Meth. B, vol. 70, pp. 276-285, 1992.
[7] P. Russotto et al., “Status and Perspectives of the INFN-LNS In-Flight Fragment Separator”, Jour. of Phys.: Conf. Ser., vol. 1014, 012016, pp. 1-12, 2018.
[8] L. Penescu et al., “Technical Design Report for a Carbon-11 Treatment Facility”, Front. Med., vol. 8, Apr. 2022, DOI: 10.3389/fmed.2021.697235.
[9] C. Altana et al., “Feasibility study of a smart rad-hard fast detection system for Radioactive Ion Beam Tagging and Diagnostics”, 2021 IEEE Nuclear Science Symposium and Medical Imain Conference Records, IEEE, 2021, pp 1-5.
[10] L. Acosta et al., “Design of a novel smart rad-hard fast detection system for Radioactive Ion Beam Tagging and Diagnostics”, 2022 IEEE Nuclear Science Symposium, Medical Imaging Conference and Room Temperature Radiation Detectors Conference Conference Records, November 5-12, 2022, Milano (Italy), pp. 1-4.
[11] S. Tudisco et al., “SiCILIA—Silicon Carbide Detectors for Intense Luminosity Investigations and Applications”, *Sensors*, vol. 18(7), 2289, pp. 1-16, 2018.
[12] A.D. Russo, L. Calabretta, G. Cardella and P. Russotto, “Preliminary design of the new FRAgment In-flight SEparator (FraISe)”, Nucl. Instrum. Meth. B, vol. 463, pp. 418-420, 2020, DOI: 10.1016/j.nimb.2019.04.037
[13] N. S. Martorana, “Status of the FraISe facility and diagnostics system”, Il nuovo cimento C, vol. 44 (1), pp. 1-10, 2021, DOI: 10.1393/ncc/i2021-21001-2
[14] N. S. Martorana et al., “Radioactive ion beam opportunities at the new FRAISE facility of INFN-LNS”, Front. Phys., Vol. 10, Dec. 2022, article n. 1058419, pp. 1-13, 2022, DOI: 10.3389/fphy.2022.1058419.
[15] https://potlns.lns.infn.it/it/

[16] J. M. Rafi' et al, "Electron, Neutron, and Proton Irradiation Effects on SiC Radiation Detectors", *IEEE Trans. Nucl. Sci*. Vol. 67, no 12, 2020, pp. 281-2489.
[17] A. Castoldi et al., "Feasibility study of the use of operational amplifiers as forward gain stages in charge preamplifiers and shaping filters for radiation detectors", IEEE Trans Nucl Sci., July 2023, DOI:10.1109/TNS.2023.3277223.